0888-8809/02/$15.00/0
Printed in U.S.A.

Molecular Endocrinology 16(12):2706–2719

doi: 10.1210/me.2002-0250

Estrogen Receptor Dimerization: Ligand Binding Regulates Dimer Affinity and Dimer Dissociation Rate

ANOBEL TAMRAZI, KATHRYN E. CARLSON, JONATHAN R. DANIELS, KYLE M. HURTH, AND JOHN A. KATZENELLENBOGEN

Department of Chemistry, University of Illinois, Urbana, Illinois 61801

Nuclear receptors form strong dimers that are essential for their function as transcription factors, and it is thought that ligand binding can affect dimer stability. In this report, we describe convenient fluorescence resonance energy transfer (FRET)-based methods for measuring the thermodynamic and kinetic stability of dimers of the estrogen receptor-α ligand-binding domain (ERα-LBD). We have developed receptors that are chemically labeled with a single fluorophore in a site-specific manner. These fluorophore-labeled ERs are functional and can be used to measure directly the affinity and stability of ERα-LBD dimers. Our results indicate that unliganded ERα-LBDs exist as very stable dimers and that the dissociation rate of these dimers is slow ($t_{1/2}$ = 39 ± 3 min at 28 C) and is further slowed ($\leq$7-fold) by the addition of various ligands. Estrogen antagonists provide greater kinetic stabilization of the ER dimers than agonists. In addition, coactivator peptides containing the LXXLL motif selectively stabilize agonist-bound ERα-LBD dimers. These fluorescence-based assays for measuring the kinetic and thermodynamic stability of ER dimers provide a functional *in vitro* method for assessing the agonist or antagonist character of novel ligands. (*Molecular Endocrinology* 16: 2706–2719, 2002)

NUCLEAR RECEPTORS (NRs) are ligand-regulated transcription factors that have a distinctive domain structure. DNA binding occurs through a small, highly conserved domain (domain C), and ligand binding, dimerization, and transcriptional activation are mediated mainly through a larger domain (domain E). NRs that bind steroid ligands (*i.e.* estrogen receptor) typically function as dimers, either homodimers between identical receptor monomers or between closely related subtypes, and NRs that bind nonsteroidal ligands typically function as heterodimers with the retinoid X receptor (RXR) (1, 2).

Dimer formation is thought to be essential for normal receptor function, because mutations that interfere with dimerization generally result in receptors that are insoluble or transcriptionally inactive (3). The principal dimerization interface of NRs is in the ligand-binding domain E and involves a large contact area that, in the case of the estrogen receptor-α (ERα), encompasses about 15% (1703 Å^2) of the surface area of each monomer (4). There is some contact between monomer units in the DNA binding domain C, but this interface is rather small, varies with different NRs, and is thought to contribute only to a minor degree to dimer stability (5).

Abbreviations: CME_2, 11-β-Chloromethyl estradiol; DES, diethylstilbestrol; E_2, 17β-estradiol; ERα-LBD, estrogen receptor-α-ligand binding domain; ERE, estrogen response element; Et-E_3, 11β-ethyl estriol; Et-EE_3, 11β-ethyl-17α-ethynyl estriol; FRET, fluorescence resonance energy transfer; GSH, glutathione Sepharose; GST, glutathione-*S*-transferase; K_d, dissociation constant; Ni-NTA, nickel nitrilotriacetic acid; NR, nuclear receptor; RAL, raloxifene; RBA, relative binding affinity; SERM, selective ER modulator; SRC, steroid receptor coactivator; TCEP, tris(carboxyethyl)phosphine; THC, tetrahydrochrysene; TOT, *trans*-4-hydroxytamoxifen.

ER has been reported to exist as a dimer even in the absence of ligand, and the dimer interaction of liganded ERα ligand binding domain (ERα-LBD) is strong and resistant to high levels of denaturants (6). ER dimers have been estimated, by indirect methods, to have an equilibrium dissociation constant (K_d) of about 2–3 nM (7), although dimer affinity varies from NR to NR (7–9). There is evidence that the strength of the dimer interaction is regulated by ligand binding, although this issue has not been studied in a systematic fashion (7–9).

In this report, we describe convenient fluorescence resonance energy transfer (FRET)-based methods for measuring the thermodynamic and kinetic stability of ERα-LBD dimers, using receptors that are chemically labeled with a single fluorophore in a site-specific manner. Using a kinetic FRET-based technique called "monomer exchange" (10), we can study the effect of ligand and coactivator binding on kinetics of ERα-LBD dimerization. We find that the rate of monomer exchange of unliganded receptor is remarkably slow and is slowed even further by ligand binding. Each class of ligand character (agonists, mixed agonist-antagonists, and pure antagonists) is found to have a characteristic effect on the rate of monomer exchange.

RESULTS

ER Mutants Having a Single Reactive Cysteine Can Be Labeled with a Cysteine-Specific Fluorophore in a Site-Specific Manner

Proteins can be covalently labeled in a site-specific manner through a reactive cysteine residue (11). The

LBD of ERα contains four cysteines: 381, 417, 447, and 530. One of these is deeply buried (C447) and is unreactive toward cysteine-specific modifying agents (12, 13), and it may be important for receptor stability, because C447A ERα has been shown to be temperature sensitive (14). Cysteine 381 has intermediate reactivity, whereas both cysteines 417 and 530 readily react with cysteine-specific modifying agents (12, 13). These studies indicate that these three residues are either partially (C381) or fully solvent exposed (C417 and C530) and are therefore candidates for site-specific labeling.

Mutational studies suggest that either a cysteine-to-alanine or a cysteine-to-serine mutation at positions 381, 417, or 530 has minimal effect on ER activity (15–19). To maintain the environment of the binding pocket, we chose serine as a conservative replacement for solvent-exposed cysteines in our constructs. To enable site-specific fluorophore labeling of the ERα-LBD, we have, in all cases, mutated cysteine 381 to serine and then separately mutated either cysteine 417 or cysteine 530 to serine, leaving a sole reactive cysteine, either at 530 or 417, respectively. For convenience, we have designated these ER constructs as ***C530*** and ***C417*** (with the *bold italic* type to indicate that they are mutant ERs with a single-reactive cysteine at that particular residue).

Our ER ***C530*** and ***C417*** constructs have an N-terminal His_6-tag through which they can be purified over nickel-nitrilotriacetic acid (Ni-NTA) resin. We found it convenient to label these ER preparations while they were attached to the Ni-NTA resin. In this manner, excess cysteine-specific fluorophore could be removed from the receptor simply by washing the resin, before elution of the receptor. We used cysteine-specific fluorophores 5-iodoacetamidofluorescein (a FRET donor) and tetramethylrhodamine-5-maleimide (a FRET acceptor). Inclusion of the nonnucleophilic thiol reductant, tris(carboxyethyl)phosphine (TCEP), to maintain the ERα-LBD in a fully reduced state, proved to be important for efficient labeling. The level of labeling, determined by matrix-assisted laser-desorption ionization mass spectroscopy (MALDI MS), was 90–95% mono labeling, with no multiple labeling evident (data not shown).

We confirmed the site of ERα-LBD labeling by analysis of the trypsin digestion pattern of receptor. Trypsin cleaves ERα-LBD at K467 to produce a 19-kDa N-terminal fragment (304–467) and a 10-kDa C-terminal fragment (468–554), the latter of which is then further cleaved to a 7-kDa fragment (468–529/531) (20, 21). When fluorophore-labeled ***C530*** ERα-LBD was treated with trypsin, only the 10-kDa and 7-kDa bands on SDS-PAGE were fluorescent, whereas when we trypsin digested ***C417*** ERα-LBD, only the 19-kDa band was fluorescent (data not shown).

The estradiol (E_2) binding affinities of unlabeled, fluorescein-, and tetramethylrhodamine-labeled ER double mutants are listed in Table 1. Previous studies have shown that ERs with single and double C-to-A, or C-to-S mutations retain near wild-type E_2 binding affinities (15–19). We have also found that our unlabeled and fluorophore-labeled C-to-S double-mutant ERα-LBDs exhibit near wild-type affinities for E_2. Interestingly, the attachment of a fluorophore to cysteine 417 or 530 appears to increase the affinity of our labeled receptors for E_2 relative to that of the unlabeled receptors (Table 1). Some of our dimer stability experiments were performed in urea (see below); therefore, we also measured E_2 binding affinity in up to 2 M urea. This concentration of denaturant causes less than a 3-fold reduction of E_2 binding affinity (Table 1), consistent with our previous investigations (Gee, A. C., and J. A. Katzenellenbogen, unpublished).

Table 1. E_2 Binding Affinities of Fluorescent ERα-LBDs

ER-LBD (304–554)	$[^3HE_2]K_d$ in buffer (nM)	$[^3HE_2]K_d$ in 2 M Urea (nM)
wt-Unlabeled	0.16	0.51
C530-Unlabeled	0.52	
C530-Acceptor	0.46	1.1
C530-Donor	0.24	0.77
C417-Unlabeled	0.58	
C417-Acceptor	0.54	1.7
C417-Donor	0.39	1.3

C417 denotes C381S/C530S double mutant. *C530* denotes C381S/C417S double mutant. Donor, Fluorescein; acceptor, tetramethylrhodamine; wt, wild-type.

To verify that the labeled ERα-LBD mutants still adopt characteristic agonist and antagonist conformations when complexed with various ligands, we performed fluorescence-based coactivator recruitment experiments. A glutathione-*S*-transferase (GST) steroid receptor coactivator-1 (SRC-1 residues 629–831, containing nuclear receptor box regions 1–3) protein construct was immobilized on glutathione Sepharose (GSH) resin and used to pull down fluorophore-labeled ERs that had been equilibrated with various ER ligands. Both ***C530***-fluorescein and ***C417***-tetramethylrhodamine receptors retain wild-type ligand-induced functional interactions with this SRC-1 coactivator peptide, with interaction being induced by agonist ligands and inhibited by antagonist ligands (Fig. 1). Thus, both the mutational changes and fluorescent labeling appear to have no detrimental effects on the characteristic activities of ER as measured by ligand binding and coactivator recruitment assay.

FRET Can Be Used to Study Ligand Effects on the Thermodynamic Stability of ERα-LBD Dimers

With donor- and acceptor-labeled receptors, we can use FRET to directly measure the thermodynamic stability (affinity) of ERα-LBD dimers. FRET develops only when an excited donor fluorophore is in close proximity to an acceptor fluorophore (typically in the range of 10–75 Å), so that it can transfer its energy (22). FRET can be followed by the enhanced emission from acceptor (at 580 nm, Fig. 2A) or by the decreased emis-

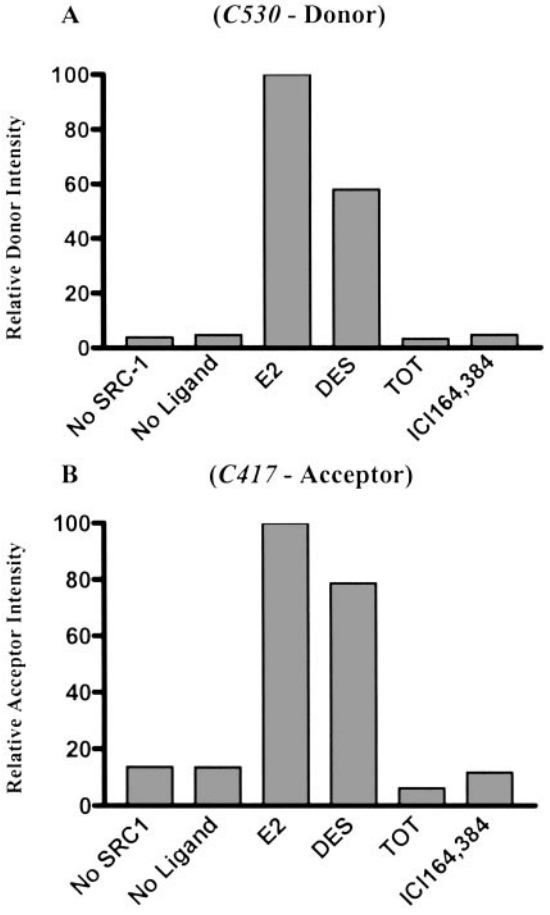

Fig. 1. GST-SRC-1 Pull Down of Fluorescent ERα-LBD Constructs

GST-SRC-1 (residues 629–831) was immobilized on GSH resin and used to pull down ligand-bound fluorescein (donor)-labeled ***C530*** (A) or tetramethylrhodamine (acceptor)-labeled ***C417*** (B) ERs. For details, see *Materials and Methods.* See Table 2 for abbreviation of ligands used.

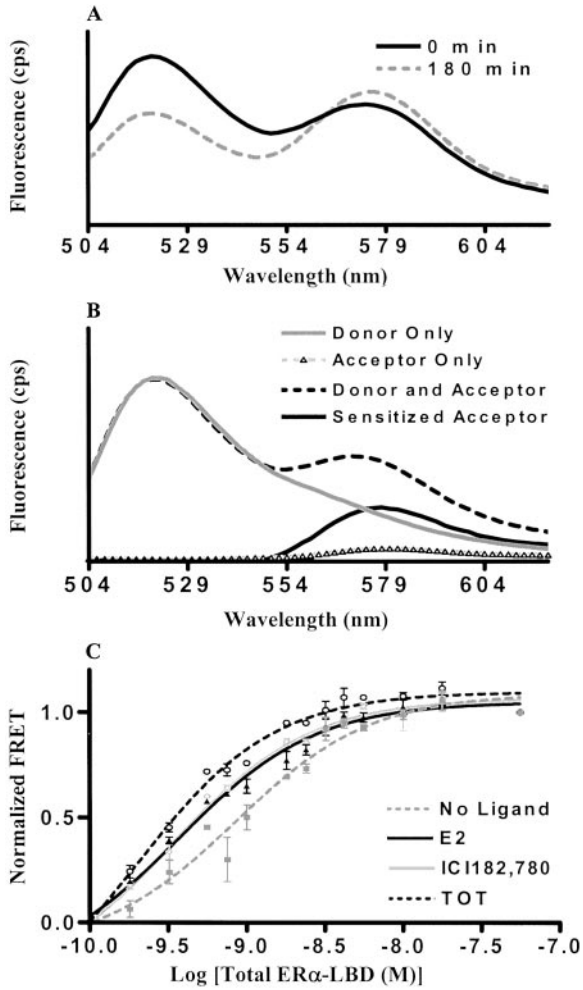

Fig. 2. FRET Between Donor- and Acceptor-ER Monomers

A, Development of a FRET signal through a decrease in donor intensity (~521 nm) and an increase in acceptor intensity (~580 nm) as donor-acceptor ERα-LBD dimers are formed. B, Donor-only and acceptor-only spectra, excited at the donor excitation (488 nm). The FRET signal through the "sensitized" acceptor emission is shown after a subtraction of donor-only spectra from the equilibrated donor-acceptor reaction. C, Thermodynamic ERα-LBD dimer affinity. All reactions conducted with 0.1 nM donor ER and titrating increasing concentration of acceptor ER with or without 1 μM ligand in 2 M urea. The calculated equilibrium dissociation constant (K_d) value for no ligand was 1.0 ± 0.2, for estradiol (E_2) was 0.33 ± 0.06, for ICI 182,780 was 0.34 ± 0.06, and for TOT was 0.27 ± 0.04. The K_d values are the mean ± SD from four similar experiments.

sion from donor (at 521 nm, Fig. 2A) (22). With the fluorophores we have chosen, donor- and acceptor-labeled ERα-LBD emission bands are broad. As a result, donor emission overlaps considerably with the acceptor maximum emission (580 nm); by contrast, there is minimal overlap of acceptor emission at the donor maximum emission (521 nm; the emission bands are shown separately in Fig. 2B). Thus, we found it is cleaner to monitor FRET as a decrease in donor intensity, rather than an increase in acceptor intensity (because the latter would require correction for the overlap of the donor emission).

To measure the K_d of ERα-LBD dimer affinity, a fixed low concentration of donor-labeled receptor (0.1 nM) was titrated with increasing concentrations of the acceptor-labeled receptor. After equilibrium was reached, FRET between donor-acceptor dimers was measured based on donor intensity (Fig. 2C). The percent FRET was then fitted to a simple single-term binding isotherm to determine the K_d (see *Materials and Methods* for details). Under native conditions (without denaturant), the K_d for the ERα-LBD dimer affinity, with or without ligand, is less than 0.1 nM (data not shown). This is below the sensitivity limit for our FRET-based method, which is limited by our ability to detect the fluorescence of donor-labeled ER. However, we found that we were able to raise the K_d of the ER dimer to the low nanomolar range by the addition of a modest concentration of a denaturant (2 M urea).

Under these equilibrium conditions, we could quantitate ligand-induced enhancement of dimer affinity (Fig. 2C).

The K_d values of ERα-LBD dimer affinity in 2 M urea (Fig. 2C) are in the absence of ligand (apo, 1.0 nM), with an agonist (E_2, 0.33 nM), a mixed agonist-antagonist [*trans*-hydroxytamoxifen (TOT), 0.27 nM], and a pure antagonist (ICI 182, 780, 0.34 nM). Under these conditions (2 M urea), there is a 3- to 4-fold increase in ERα-LBD dimer affinity with these three ligands of different character.

FRET Can Be Used to Study the Kinetic Stability of ERα-LBD Dimers

In the absence of denaturant, the ERα-LBD dimer affinity is quite high ($K_d < 0.1$ nM), and, as noted above, this makes it technically challenging to measure ligand effects on thermodynamic dimer stability using FRET under native conditions. Hence, to measure dimer stability under native conditions, we used a standard kinetic FRET technique termed "monomer exchange" (Fig. 3 and Ref. 10).

Monomer exchange is conducted by mixing a preparation of donor-labeled dimers with a preparation of acceptor-labeled dimers and monitoring the development of FRET with time, as donor-acceptor dimers are formed. In our experiments, the rate at which a FRET signal develops is governed by the rates at which donor-donor homodimers and acceptor-acceptor homodimers dissociate into monomers and then reassociate to form donor-acceptor heterodimers (Fig. 3). We have found, as expected, that monomer exchange kinetics do not change with increasing excess of acceptor-labeled receptor, which indicates that dimer dissociation (rather than monomer reassociation) is the rate-determining step of this process (data not shown) (10). Thus, the monomer exchange kinetics we observe with fluorescent receptor is an accurate measure of the rate of dimer dissociation and hence represents the kinetic stability of the ERα-LBD dimer.

A representative dimer kinetic stability experiment is shown in Fig. 4A. To maximize the FRET signal (in our experiments typically 35–50%) we used a 4:1 ratio of acceptor to donor receptor, so that every donor-labeled monomer is more likely to find an acceptor-labeled monomer. To confirm that the FRET signal results from the formation of donor-acceptor dimers, we determined that we could abrogate the FRET signal by adding an excess of unlabeled ER, which would then undergo monomer exchange and disrupt the donor-acceptor dimers (data not shown).

The rate of monomer exchange for apo (no ligand) ERα-LBD is slow (half-life of 39 $\pm$ 3 min at 28 C), indicating that ERα-LBD dimers are stable in the absence of ligand. In experiments where a ligand was used, we equilibrated donor-donor and acceptor-acceptor homodimers separately with sufficient ex-

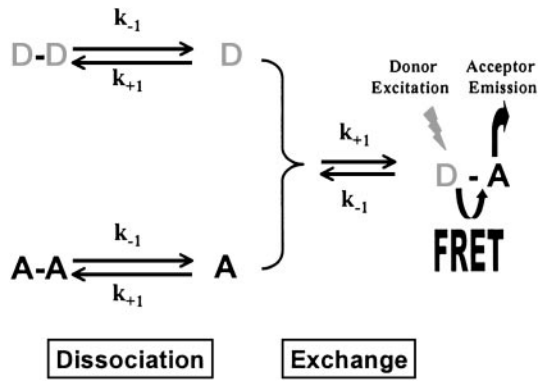

Fig. 3. Scheme Representing the Kinetics of Monomer Exchange

D denotes donor (fluorescein)-labeled ER, A denotes acceptor (tetramethylrhodamine)-labeled ER, k_{-1} and k_{+1} are the dissociation and association rates, respectively. Donor- and acceptor-labeled ER preparations incubated with the same ligand were mixed, and the kinetics of monomer exchange was monitored with time as a FRET signal developed when a donor-acceptor dimer formed.

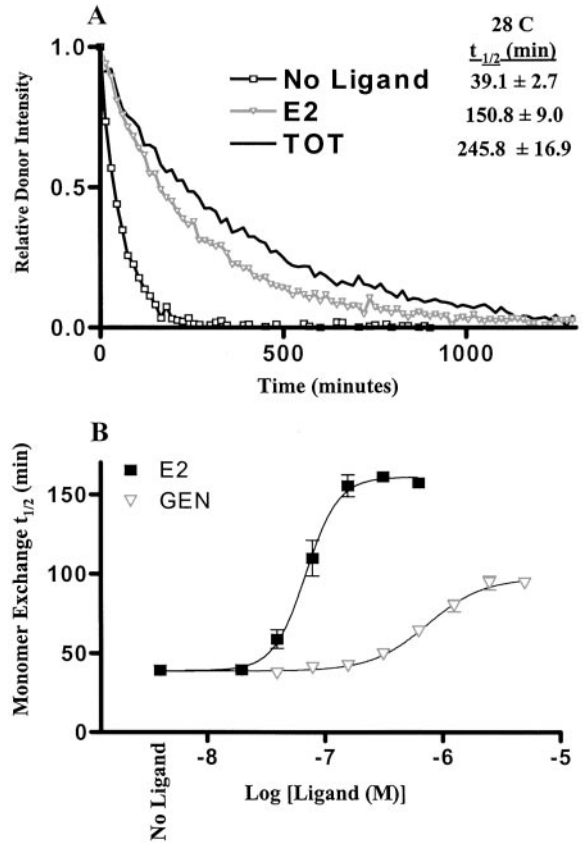

Fig. 4. Dimer Kinetic Stability of ERα-LBD

A, Dimer dissociation kinetics of ERα-LBD with or without 1 μM ligand was monitored through the generated FRET signal by following donor intensity with time at 28 C. B, The effects of ligand binding on ERα-LBD dimer kinetic stability. Dimer dissociation half-life increases and reaches a limiting value as a function of receptor ligand occupancy. Results are indicative of two similar experiments. GEN, Genistein.

cess of the same ligand for sufficient time to fully saturate these receptors and then mixed them to initiate the monomer exchange process (see *Materials and Methods* for details). Compared with apo receptor, the rate of monomer exchange is slower (an indication of more stable dimers) in the presence of saturating concentrations of most ligands. In Fig. 4A, E_2 (slowed 3.8-fold) and the selective ER modulator (SERM), TOT (slowed 6-fold) are shown.

Ligand Binding Affects the Kinetic Stability of ERα-LBD Dimers

Titration experiments allowed us to estimate ligand concentrations that fully saturate the receptor (Fig. 4B). Here, the EC_{50} values reflect relative ligand affinity, whereas, the efficacy of dimer kinetic stability (*i.e.* maximum half-life under saturating ligand conditions) indicates the degree to which a particular ligand induces a conformation that stabilizes the dimer. Shown in Fig. 4B are both a high-affinity ligand [E_2, relative binding affinity (RBA) 100%] and a low-affinity ligand (genistein, RBA 0.013%). The rate of monomer exchange becomes progressively slower as receptor becomes occupied and reaches a maximum at ligand saturation (Fig. 4B). All monomer exchange experiments were conducted under saturating ligand conditions (1 μM for most ligands, and 5 μM for very-low-affinity ligands).

Using our convenient FRET-based dimer kinetic stability assay, we have systematically assessed more than 30 natural and synthetic ligands for their effects on dimer dissociation of ERα-LBDs. As agonist ligands, we have used estrogens, phytoestrogens, and synthetic agonists having various RBAs (Table 2). As mixed agonist-antagonist ligands, we have used raloxifene (RAL), TOT, tamoxifen, cyclofenil, and three of our novel ER subtype-selective antagonist ligands (furan propyl antagonist, furan ethyl antagonist, and pyrazole ethyl antagonist) (Table 2 and Refs. 23–25). Additionally, as pure antagonists, we have used ICI compounds ICI 182,780 and ICI 164,384.

All dimer dissociation results with various ligands and ERα-LBD are summarized in Table 3. Our studies show that not all agonists alter the ERα-LBD dimer dissociation kinetics to the same degree (Fig. 5A). Compared with the apo receptor, different agonist ligands affect the dimer dissociation kinetics by factors that range from 0.65- to 6.2-fold. The endogenous agonist, E_2, increased dimer kinetic stability by 3.8-fold, and the highly potent agonist, 11β-chlolomethyl E_2 (CME_2) (26), causes a 5-fold increase in dimer stability (Fig. 5A). Certain agonists [tetrahydrochrysene (THC)-ketone, R,R- and S,S-THC], by contrast, afford no stability to ERα-LBD dimers or actually destabilize them (Fig. 5A), yet they are known to be agonists on ERα and are capable of inducing a conformation in the LBD that is effective in recruiting coactivators (27, 28). Interestingly, these THC-based ligands exhibit a range of cell type-specific ER transcriptional efficacies, which are, in some cases, lower than with E_2 (Katzenellenbogen, B. S., unpublished results). Mixed agonist-antagonist ligands showed, in general, an even greater effect than agonists (4.5- to 7-fold), but within a narrower range. Compared with mixed agonist-antagonists, the pure antagonist ICI compounds had a somewhat lesser dimer stabilizing effect (3.5- to 4.5-fold relative to apo receptor; Fig. 5B). A structural hypothesis that might account for these observations will be presented in *Discussion*.

Dimer Kinetic Stability Reflects Ligand Character, Not Affinity

We next asked whether an increase in ER dimer stability is simply a reflection of ligand affinity for the receptor, or does ligand character play a key role in ERα-LBD dimer stability? To examine the relationship between ligand affinity and dimer kinetic stability, we compared the log of the RBAs from Table 2 with the log of dimer dissociation rates of ER-ligand complexes from Table 3. This comparison showed no correlation between ligand affinity and dimer dissociation rate (data not shown). Furthermore, dimer dissociation rates do not appear to be a simple reflection of ligand dissociation rates (an additional measure of ligand affinity separate from RBA), which we have reported previously by both radiometric and fluorescence-based assays (26, 29, 30).

Our novel furan and pyrazole ligands, which are available in both agonist and antagonist forms within a structurally homologous series, enable us to investigate the issue of dimer stability and ligand character. Interestingly, the ERα-LBD dimer stability is lower for the higher-affinity furan and pyrazole agonists than it is for their corresponding lower-affinity antagonists (Table 2 and Fig. 5). This suggests that dimer kinetic stability appears to be more a function of ligand character (*i.e.* agonist *vs.* antagonist) than ligand affinity or ligand core structure. This trend is also seen with the generally greater dimer stability of ERα when it is bound with traditional antagonist *vs.* agonist ligands and is supported by an earlier report in which a chromatographic technique was used to monitor the rate of wild-type ERα-LBD monomer exchange (7).

Some interesting structure-activity relationships were observed from the ligands monitored for dimer kinetic stability effects on ERα-LBD (Fig. 5). The presence of a basic side chain (piperidine or dimethylamino-ethoxy) on antagonist ligands caused a substantial increase in dimer kinetic stability compared with structurally similar ligands (agonists) lacking this basic side chain [furan and pyrazole series; also tamoxifen and TOT *vs.* diethylstilbestrol (DES)]. Additionally, an 11β substituent enhanced dimer kinetic stability compared with a similar ligand lacking a substituent at this position [CME_2 *vs.* E_2, or 11β-ethyl estriol (Et-E_3) *vs.* E_3]. The addition of a 17α-ethynyl group decreases dimer stability in the estriol series,

Table 2. Structures and RBA[a] Values of the Ligands Surveyed

Ligand	Structure	Ligand	Structure	Ligand	Structure
Estradiol (E_2) (100)	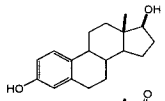	Cyclofenil (151)	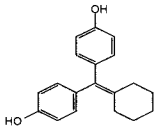	R,R-THC (3.6)	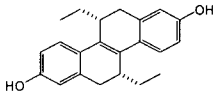
Estrone (E_1) (4.64)	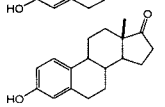	Tamoxifen (0.89)	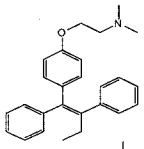	S,S-THC (0.79)	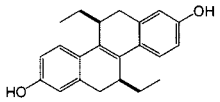
Estriol (E_3) (7.10)	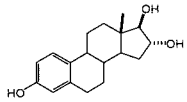	Trans-hydroxy-tamoxifen (TOT) (144)	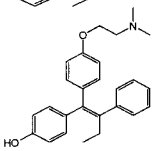	THC-Ketone (69.3)	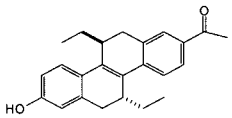
11β–chloromethyl-estradiol (CME_2) (206)	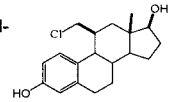	Raloxifene (RAL) (41.2)	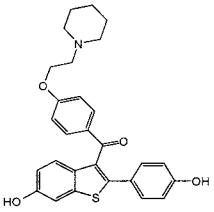	Propyl-Pyrazole-Triol (PPT) (89.1)	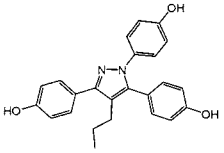
11β-ethyl-estriol (Et E_3) (26.3)	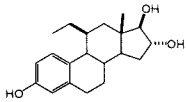	Genistein (GEN) (0.013)	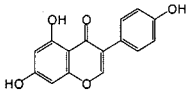	Pyrazole Ethyl Agonist (Pyr. Et. Agonist) (61.7)	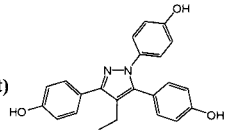
11β-ethyl-17α-ethynyl-estriol (Et EE_3) (71.3)	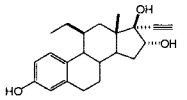	P1496 (9.77)	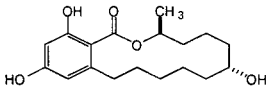	Furan Ethyl Agonist (Furan Et. Agonist) (166)	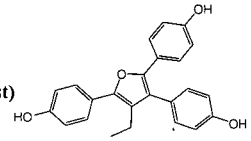
ICI 182,780 (79.4)	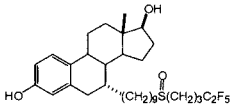	P1498 (12.3)	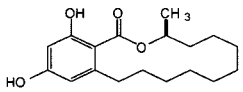	Pyrazole Ethyl Antagonist (Pyr. Et. Antag.) (23.3)	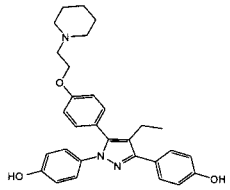
ICI 164,384 (97.7)	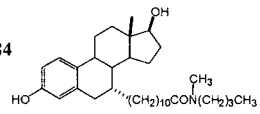	β-Zearalenol (0.032)	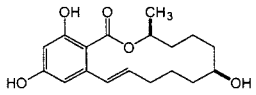	Furan Propyl Antagonist (Furan Pr. Antag.) (45.0)	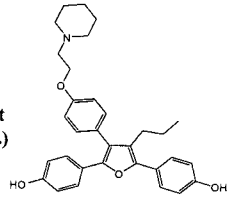
Diethylstilbestrol (DES) (219)	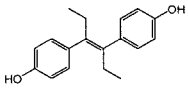	o,p'-DDT (0.025)	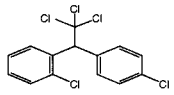	Furan Ethyl Antagonist (Furan Et. Antag.) (52.4)	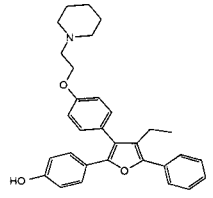
Hexestrol (270)	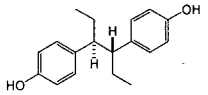	Trans-Diethyl-THC (Trans. E. THC) (141)	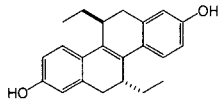		
Benzestrol-B2 (114)	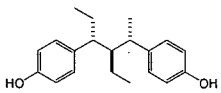				

[a] The binding affinities are presented *in parentheses* and are expressed relative to the binding of estradiol, which is set at 100. Similar RBA values were obtained with these compounds using our ERα-LBD and full-length ERα purchased from PanVera (Madison, WI).

Table 3. ERα-LBD Monomer Exchange Rates under Saturating Ligand Conditions

Ligand	Agonists		n	Ligand	Antagonists		n
	k (min^{-1})[a]	$t_{1/2}$ (min)			k (min^{-1})[a]	$t_{1/2}$ (min)	
No ligand	0.0178 ± 0.0012	39 ± 3	16				
THC-ketone	0.0260 ± 0.0027	27 ± 3	4	ICI164,384	0.0051 ± 0.0003	137 ± 9	8
S,S THC	0.0189 ± 0.0016	37 ± 3	8				
R,R THC	0.0154 ± 0.0051	50 ± 17	8	ICI182,780	0.0042 ± 0.0003	165 ± 11	8
Benzestrol (B2)	0.0116 ± 0.0002	60 ± 1	3				
Furan Et. agonist	0.0102 ± 0.0003	68 ± 2	4				
Pyr. Et. agonist	0.0101 ± 0.0007	69 ± 5	8				
βZearalenol	0.0096 ± 0.0006	73 ± 5	4				
PPT	0.0088 ± 0.0008	80 ± 8	4	Pyr. Et. Antag.	0.0040 ± 0.0002	173 ± 10	8
Hexestrol	0.0078 ± 0.0008	90 ± 9	4				
o,p DDT	0.0076 ± 0.0008	93 ± 11	2[b]	Furan Pr. Antag.	0.0040 ± 0.0002	174 ± 8	4
Gen	0.0074 ± 0.0003	94 ± 4	2[b]				
p1498	0.0068 ± 0.0003	102 ± 4	4	Tamoxifen	0.0038 ± 0.0001	184 ± 4	6
Trans. E. THC	0.0064 ± 0.0004	109 ± 7	9				
DES	0.0062 ± 0.0009	113 ± 14	4	Cyclofenil	0.0033 ± 0.0001	209 ± 7	4
E_3	0.0058 ± 0.0002	121 ± 5	4				
p1496	0.0048 ± 0.0003	146 ± 9	4	Ral	0.0030 ± 0.0001	232 ± 12	4
E_1	0.0046 ± 0.0001	150 ± 4	4				
E_2	0.0046 ± 0.0003	151 ± 9	8	TOT	0.0028 ± 0.0002	246 ± 17	8
Et-EE_3	0.0040 ± 0.0001	174 ± 6	4				
CME_2	0.0033 ± 0.0002	209 ± 10	8	Furan Et. Antag.	0.0025 ± 0.0001	278 ± 4	4
Et-E3	0.0029 ± 0.0001	242 ± 7	4				

Et., Ethyl; Pyr., pyrazole; PPT, propyl pyrazole triol; DDT, dichlorodiphenyltrichloro-ethane; Gen, genistein; DES, diethylstilbestrol.
[a] k denotes the single exponential decay rate for monomer exchange, values are the mean ± SD (or range when n = 2).
[b] Denotes rates determined by ligand titration experiments up to 5 μM ligand, similar to Fig. 4B. n is the number of experiments. For details, see *Materials and Methods.* See Table 2 for abbreviation of ligands used.

although it increases ligand binding affinity [11β-ethyl-17α-ethynyl estriol (Et-EE_3) *vs.* Et-E_3].

Coactivator Peptides Selectively Stabilize Agonist-Bound ERα-LBD Dimers and Provide a Functional Assay to Identify Ligand Character Based on Dimer Stability

Our FRET-based monomer exchange assay provides a convenient measure of ligand-induced dimer kinetic stability in a highly purified *in vitro* model system. Having obtained an initial structure-activity relationship profile of ligand-induced ER dimer stability, we wanted to see whether coactivator peptides, which should bind only to agonist-ER complexes, would enhance and sharpen the structure-activity relationship. Additionally, coactivators are present in *in vivo* systems; therefore, adding them to our *in vitro* model system makes it more similar to the *in vivo* situation.

The addition of a coactivator peptide containing residues 629–831 of SRC-1 (encompassing LXXLL NR boxes 1–3) or of a 15-residue peptide containing only the NR box-2 of SRC-1 coactivator protein, caused up to a 2-fold kinetic stabilizing effect on E_2-ERα-LBD dimers (Fig. 6A). In terms of this effect, the longer SRC-1 fragment containing three NR boxes has a potency (EC_{50}) about 100-fold higher than the single NR box-2 peptide of SRC-1. Both coactivator peptides, as expected, failed to stabilize antagonist-bound ERα LBD (ICI 182, 780-ERα-LBD dimers, as shown in Fig. 6B). Thus, the coactivator peptide-enhanced ER dimer stabilization is highly selective for agonist-bound receptor (Fig. 6C). To our knowledge, this is the first direct evidence for coactivator-mediated nuclear receptor dimer stabilization. A mechanistic rationale for this process will be presented in *Discussion*.

Addition of 10 μM NR box-2 peptide of SRC-1 (~10-fold above the EC_{50} for the E_2-ERα-LBD dimers, Fig. 6A), which stabilized agonist- but not SERM- or pure antagonist-occupied receptor dimers, caused a decrease in the kinetic stability of apo ERα-LBD dimer (Fig. 6C). The LXXLL sequence motif of NR box regions is hydrophobic and resembles the leucine-rich motif of the ERα dimer interface of helices 10 and 11. Therefore, the NR box peptide could be destabilizing the weaker apo receptor dimers by mimicking this region of the dimer interface. Recently, Yudt *et al.* (31) reported similar ERα-LBD dimer-disruptive effects by a leucine-rich 16-residue peptide. Conducting our convenient monomer exchange experiments at coactivator peptide concentrations about 10-fold above the EC_{50} of E_2-ERα-LBD dimer stability enables us to separate apo receptor from agonist- and antagonist-bound receptor complexes (Fig. 6C).

DISCUSSION

Dimer stability of nuclear receptors is an important issue, because it is considered to be a key step in NR action. In this report, we present a FRET-based

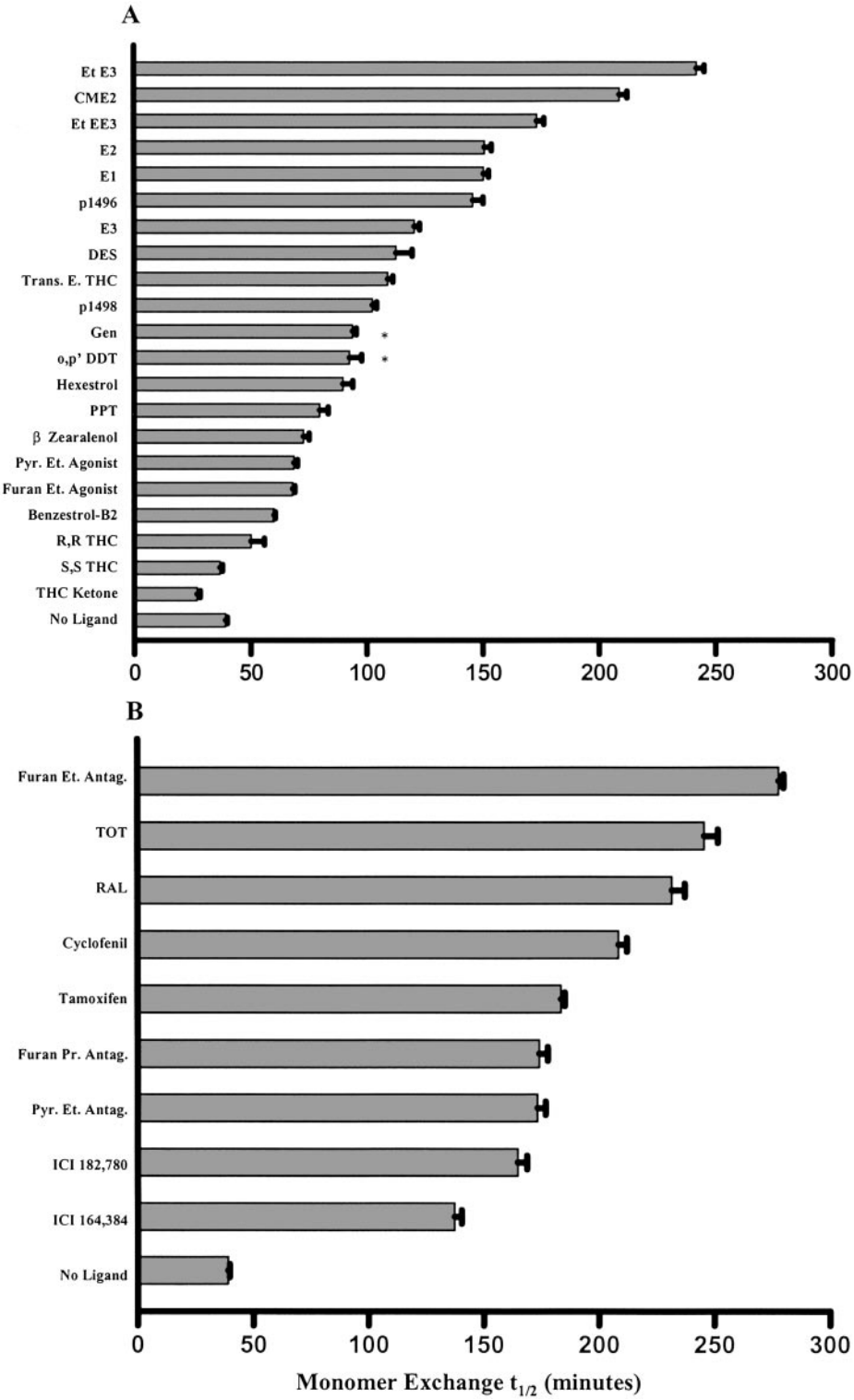

Fig. 5. The ERα-LBD Dimer Dissociation Half-Life Values in the Presence of Saturating Ligand Concentration

A, Apo and agonist ligand profile. B, Apo and mixed agonist-antagonist and pure antagonist profile. *, Half-lives determined under 5 μM ligand concentration. See Table 2 for abbreviation of ligands used.

method for measuring the stability of ERα dimers, using ERα-LBDs that are singly labeled with either fluorescein or tetramethylrhodamine, in a site-specific manner, on cysteine 417 or 530. We have used this system to study the effects of various ligands and coactivator peptides on the thermodynamic and ki-

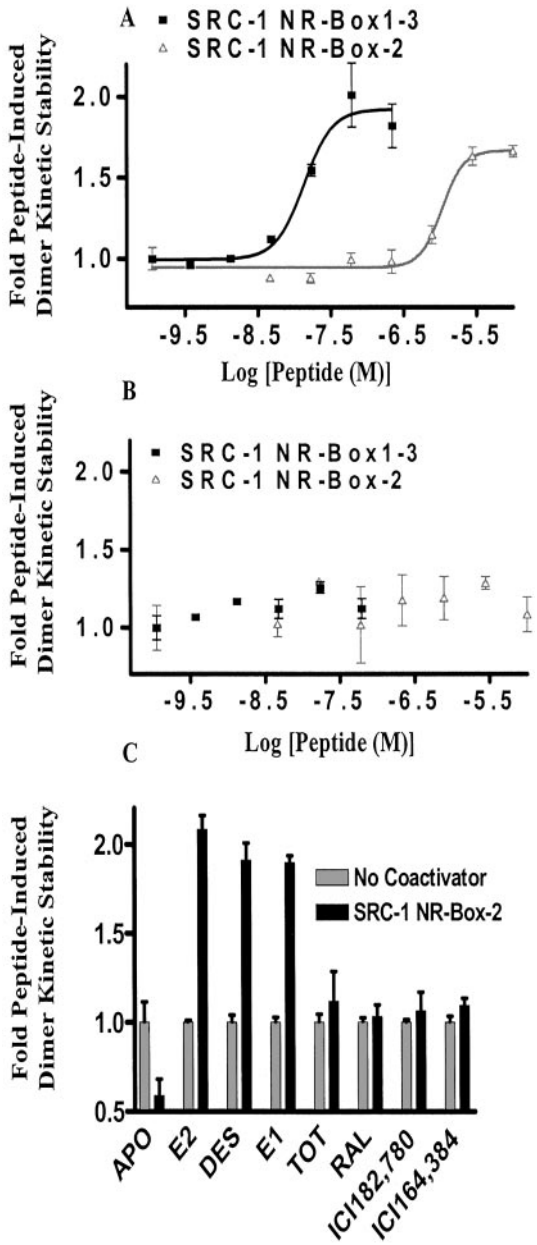

Fig. 6. Coactivator Peptide-Mediated Agonist-ER Dimer Stability

A, The effects of increasing concentration of coactivator peptides on E_2-ERα-LBD dimer kinetic stability, results normalized to dimer dissociation rates in the absence of peptide. B, Similar titration to panel A, but in the presence of the pure antagonist ICI 182,780. C, The effect of 10 μM SRC-1-NR Box-2 peptide on dimer kinetic stability of ERα-LBD with various ligands. Values are expressed as fold enhancement of dimer kinetic stability in the presence of coactivator peptide. Results are indicative of three similar experiments.

netic stability of ER dimers, in solution and under equilibrium conditions. We find that most ligands stabilize ER dimers, with antagonist ligands having a generally greater stabilizing effect than agonists, although within each class of ligand character a spectrum of stabilization factors was obtained. Coactivator peptides selectively stabilize only agonist-bound ERα-LBD dimers, and this effect can be used to define the agonist *vs.* antagonist character of new ER ligands. Our FRET-based dimer stability assays are convenient and can be developed into high throughput methods.

The site-specific labeled, fluorescent ERα-LBD double C-to-S mutants that we have prepared have shown near wild-type characteristics in ligand binding and coactivator recruitment studies (Table 1 and Fig. 1), consistent with reports of full-length ERs with multiple cysteine-to-alanine or cysteine-to-serine mutations also maintaining near wild-type binding affinity and transcriptional activity (17, 18). Curiously, the unlabeled cysteine-to-serine mutants have lower binding affinity than the labeled mutants (Table 1). Others have reported lower affinity in these mutants and have ascribed this to a change in the overall lipophilic balance of ER (change in protein hydration due to C-to-S mutations) (18). Perhaps, addition of the lipophilic fluorophore to the remaining reactive cysteine restores the lipophilic balance of ER that has been perturbed by the cysteine-to-serine mutations.

Site-Specific Fluorophore-Labeled ERα-LBDs Enable the Direct Measurement of ER Dimer Stability and Ligand-Induced Changes in This Stability

Using our donor- and acceptor-labeled ERα-LBD constructs in a FRET-based dimer formation assay, we have measured directly the dimer affinity of apo and ligand-bound receptors, under equilibrium conditions. To our knowledge, this is the first report showing a direct measurement of ER dimer affinity, and we find that the K_d for dimerization is much lower ($<$0.1 nM) than the previously reported values measured using indirect techniques (6, 7). In fact, due to technical limitations, we could not determine the K_d in the absence of denaturants. This very high receptor dimer affinity is consistent with the highly hydrophobic nature of the dimer interface (helices 10 and 11 of ERα-LBD) (4, 6, 32).

Under mild denaturing conditions (2 M urea, which causes only about a 3-fold loss in E_2 binding affinity, Table 1), we could investigate how ligands of various agonist *vs*. antagonist character affect dimer affinity (Fig. 2C). We find that E_2-, ICI 182,780-, and TOT-occupied receptors have a 3- to 4-fold higher dimer affinity compared with apo ERα-LBD dimers (Fig. 2C).

Using a different FRET-based assay, a monomer exchange assay, we have made a careful analysis of kinetic stability of the ERα-LBD dimer and how this is affected by ligands having a broad range of affinity, structure, and agonist *vs*. antagonist character (Fig. 5 and Table 2). The results indicate that the rate of dimer dissociation, which presumably reflects the manner in which the conformation of the ER-ligand complex affects the dimer interface, is not a simple function of ligand binding affinity, or ligand dissociation kinetics,

but more reflects ligand character. In general, and especially where specific comparisons can be made (*e.g*. with structurally related pyrazole and furan agonists and antagonists), it appears that antagonists stabilize the ERα dimer more than do agonists. The degree of dimer stabilization within each class of ligand character, however, covers a range of values.

This large range (0.65- to 6.2-fold) of ligand-induced kinetic stabilization of ERα-LBD dimers, encountered with steroidal estrogens, phytoestrogens, and nonsteroidal estrogens (all of which are considered to be agonists), may play a significant role in determining the lifetime of the ER dimer when it is bound to an estrogen response element (ERE) in a transcriptionally active complex in association with other downstream factors. The lifetime of this complex could be important in determining the *in vivo* potency and efficacy of a particular ligand and the selectivity with which it is capable of inducing the various biological responses that are regulated by ER.

In our FRET-based monomer exchange assay, the SERMs (TOT, RAL) and our furan and pyrazole antagonist ligands showed consistently higher dimer kinetic stability compared with E_2 and the majority of other agonist ligands surveyed (Fig. 5). Interestingly, two-hybrid ER dimerization studies performed *in vivo* suggest the opposite, namely, that the dimers of agonist-bound receptors are more stable than those of antagonist-bound ones (9). This discrepancy could be due to the presence of endogenous coactivator proteins containing LXXLL sequence motifs within the cellular context of the *in vivo* studies. We have, in fact, observed that SRC-1 coactivator peptides selectively stabilize only agonist-bound ER dimers (Fig. 6). Hence, our *in vitro* studies, which are performed using highly purified receptor in the absence of other interacting proteins, may provide a clearer picture of ligand-induced effects on receptor dimer structural stability. They do suggest that coactivator content of different tissues could play a role in the kinetic stabilization of transcriptionally active ER dimers, which, in turn, may offer an explanation for the complex tissue-selective pharmacology observed with ER ligands.

Structural Considerations May Account for the Different Effects of Agonists, SERMs, and Pure Antagonists on ERα-LBD Dimer Kinetic Stability

The greater kinetic stability of ERα-LBD dimers that is engendered by mixed agonist-antagonists might be due to two factors: 1) the dimer interface or contact region is enlarged and hence more stable in the ER antagonist complexes; and/or 2) ER conformational changes outside of the dimer interface result in the active destabilization of the ER agonist structures. We have examined both of these possibilities through modeling.

An overlay of the E_2- (an agonist, *green*) and TOT-bound (a mixed agonist-antagonist, *red*) ERα-LBD x-ray structures show that the two structures of ERα-LBD overlay well, especially in the dimer interface region of helices 10 and 11 (Fig. 7A). Thus, from these structures there is no evidence of an enlarged/stabilized dimer interface in the antagonist ER structures, although it is possible in solution, where ER conformations are more dynamic, that this is the case.

The other possibility is that in the agonist-bound ER conformation there may be a competing dimer-destabilizing effect, which renders the dimer dissociation

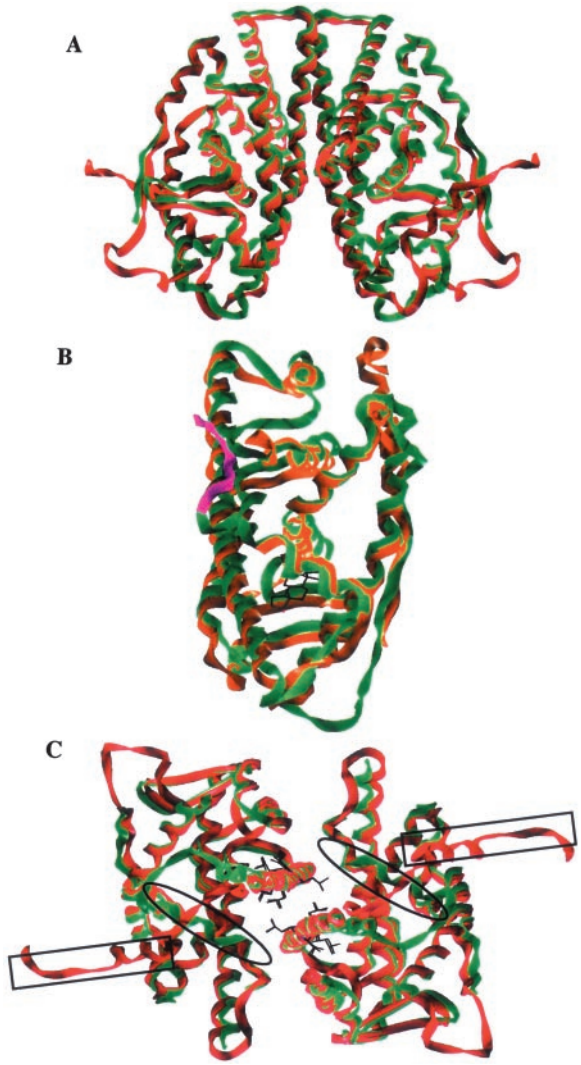

Fig. 7. Structural Rationale for the Enhanced Dimer Stability Mediated by the SERMs

A, Overlay of E_2 [*green* (4)] and TOT [*red* (32)] bound ERα-LBD dimers. B, Overlay of E_2-ERα-LBD monomer (*orange*) and agonist-bound androgen receptor-LBD [*green* (33)] with the C-terminal dimer disruptive region highlighted in *purple*. C, A 90-degree rotated view of the overlay from panel A, with the agonist and antagonist conformations of helix 12 highlighted with *ovals* and *rectangles*, respectively. Also some of the key dimer interface residues along helices 10 and 11 are shown in *black*. Figures were generated with Sybyl 6.7 from the corresponding research collaboratory for structural bioinformatics protein data bank (RCSB-PDB) files, 1ERE, 3ERT, and 1I37.

process more rapid with these ligands. Sack *et al.* (33) showed by x-ray structural analysis that wild-type androgen receptor-LBD bound to an agonist is a monomer. In this structure, the residues C terminal of helix 12 project into the region that is normally the dimer interface and thus appear to actively block dimerization. An overlay of the E_2-bound ERα-LBD monomer (*orange*) with this monomeric androgen receptor (*green*) reveals how residues C terminal of the ER helix 12 might have a similar dimer-disrupting effect in agonist-bound ER conformations (Fig. 7B). A close comparison of ER crystal structures show that the residues C terminal of helix 12 are indeed positioned in close proximity to the dimer interface in the agonist (*ovals*), but are far from this interface in the antagonist (*rectangles*) structures of the ERα-LBD (Fig. 7C). Although our ERα-LBD construct (residues 304–554) lacks the F domain of ER, it does contain a few residues C-terminal to the end of helix 12, which are not resolved in the x-ray crystal structures of agonist-bound ERs. Thus, these residues could be playing a disruptive role on the dimer stability of agonist-bound ERα-LBD complex in solution. In addition, *in vivo* experiments have shown that these same C-terminal residues in the ER may play a role in dimer destabilization, although it is uncertain whether ligand character differentially affects this process (34).

Previous studies have suggested a possible dimer disruption and high cellular turnover rate effected by the ICI antiestrogens on full-length ER (35). Our dimer kinetic stability assays show that the ICI compounds engender the most rapid monomer exchange rates of all antagonists and SERMs surveyed (Fig. 5B). They cause about 35% less kinetic stabilization of ERα-LBD dimers compared with the SERMs (TOT and RAL). Pike *et al.* (36) recently reported the x-ray crystal structure of ICI 164,384-bound ERβ-LBD, in which helix 12 is not resolved and is therefore highly mobile. Thus, in the ICI structure, the residues C terminal of helix 12 might have a dimer-destabilizing effect that is intermediate between that of the agonist ligands (active destabilization enforced by the agonist position of helix 12 pointed toward the dimer interface) and the SERMs (active destabilization prevented by helix 12 being in the extended antagonist position pointing away from the dimer interface). This could account for the more modest effect of the ICI pure antagonists on stabilizing the ERα-LBD dimers.

This structural model provides a satisfying rationale for the different degrees to which agonists, mixed agonist-antagonists, and pure antagonists stabilize ER dimers, in general. The fact that the dimer stabilities observed within each of these three classes overlap one another, however, suggests that a factor that is specific to the ligand, irrespective of its pharmacological class, is involved. We can only speculate that the different ligand structures of the members within each of these biocharacter classes have subtle effects on the conformation of the dimer interface that contribute to dimer stability.

Changes in the receptor conformation could differentially influence the dimer stability of activated receptors (agonist-bound) and could be a possible innate mechanism to turn off these receptors, so as to maintain homeostasis in the cell. To evaluate this hypothesis, we are currently working toward generating fluorescent ERα constructs with both E and F domains.

Using Coactivator-Induced Dimer Stability to Define Ligand Agonist *vs.* Antagonist Character

In addition to gaining insight into ligand-induced perturbation in ERα-LBD dimer interface structure and function, our convenient FRET-based monomer exchange assay can also be used to define the agonist *vs*. antagonist character of previously uncharacterized ligands. We have found that coactivator peptides selectively increase the dimer kinetic stability of agonist-bound ERα-LBD receptors (Fig. 6) in a manner that clearly distinguishes them from antagonist-bound ERs. This selective increase in dimer kinetic stability is reminiscent of the effect that coactivator peptides have of reducing the agonist ligand dissociation rate, as demonstrated previously in our laboratory (30).

In recent studies, it has been reported that of the first three NR box regions of SRC-1, box-2 has the highest affinity for E_2-, diethylstilbestrol-, or genistein-bound ERα (37). When compared in our coactivator-enhanced dimer stability studies, the multivalent SRC-1 peptide (NR boxes 1–3) shows about a 100-fold higher potency (EC_{50}) compared with the single NR box-2 peptide (Fig. 6A). We and others have shown that there is a 1:1 stoichiometry between a nuclear receptor LBD dimer and a multivalent SRC-1 peptide, using solution and x-ray techniques (30, 38, 39). Thus, the higher potency of the longer SRC-1 peptide, in terms of increasing the kinetic stability of agonist-bound receptor dimers, might be caused by a dimer-tethering effect, induced by this multivalent coactivator peptide. The presence of multiple NR boxes within many coactivator proteins could be part of an integral mechanism whereby these multivalent proteins tether activated NR dimers and increase their kinetic stability. Regardless of the exact mechanism of this stabilization, either coactivator peptide (SRC-1-NR boxes 1–3, or SRC-1-NR box-2) will separate agonist from antagonist ligands in our dimer kinetic stability assay, thus providing a definitive identity to the character of any novel ER ligand.

Fluorescent Nuclear Receptors: Probes for Monitoring Structure and Biological Functions

It is not clear whether ligands affect dimer stability of other NRs, such as the androgen and progesterone receptors (8, 33). Many steroid, nonsteroid, and orphan NRs have a low number of conserved cysteine residues in their LBDs (generally three to five cysteines per LBD) (8). Thus, the methodology that we have developed for ERα should be applicable, as well, to

the study of ligand-induced effects on dimer affinity and monomer exchange dynamics in these other NR systems.

We are in the process of using fluorescent ERβ-LBDs to study homo- and heterodimers of both ER subtypes and the manner in which SERMs and ER subtype-selective ligands (both agonists and antagonists) modulate differential homo- and heterodimer stability. Fluorophore-labeled ERs can also be used for the development of other types of assays to characterize receptor conformation, conformational dynamics, and ligand or coregulator interactions.

MATERIALS AND METHODS

Materials

Radiolabeled E_2 ([^{3}H]E_2) ([6,7-^{3}H]estra-1,3,5, (10)-triene-3,17-β-diol), 54 Ci/mmol, was obtained from Amersham Pharmacia Biotech Biosciences (Piscataway, NJ). Isopropyl-β-D-thiogalactopyranoside, imidazole, β-mercaptoethanol, E_2, ampicillin, estrone, estriol, genistein, *o,p′*-dichlorodiphenyltrichloro-ethane, hexestrol, tamoxifen, α-Zearalanol (P1496), and TOT were obtained from Sigma (St. Louis, MO). P1498 and β-Zearalenol were obtained from International Minerals and Chemical Corp. (Terre Haute, Indiana). Cyclofenil, raloxifene, furan propyl antagonist, furan ethyl antagonist, furan ethyl agonist, pyrazole ethyl antagonist, pyrazole ethyl agonist, propyl pyrazole triol, *trans*-diethyl-THC, S,S-THC, R,R-THC, THC-ketone, benzestrol (B2), diethylstilbestrol, Et-EE_3, and Et-E_3 were synthesized in our laboratory (24, 25, 28, 40). ICI 164,384 was a gift from Dr. Alan Wakeling and ICI Pharmaceuticals (Macclesfield, UK); ICI 182,780 was purchased from Tocris Cookson, Inc. (Ballwin, MO); CME_2 was a gift from Organon (Oss, The Netherlands). TCEP, tetramethylrhodamine-5-maleimide and 5-iodoacetamidofluorescein were purchased from Molecular Probes, Inc. (Eugene, OR). DNA primers were purchased from Bio-Synthesis, Inc. (Lewisville, TX). QuikChange Site-Directed Mutagenesis Kit was purchased from Stratagene (La Jolla, CA). Ni-NTA resin was purchased from QIAGEN (Valencia, CA). Full-length ERα was purchased from PanVera. The pET-15b vector and competent BL21 (DE3)pLysS *Escherichia coli* were obtained from Novagen. For this study we have used two fluorometers to monitor fluorescence in our experiments: a Spex Fluorolog II (model IIIc) cuvette-based fluorometer with Data Max 2.2 software (Jobin Yvon, Inc., Edison, NJ), and a Gemini XS plate reader with Soft max Pro 3.1.2 software (Molecular Devices, Inc., Sunnyvale, CA). All data were analyzed using Prism 3.00 (GraphPad Software, Inc., San Diego, CA). The RBA of the ligands was determined in wild-type ERα-LBD and baculovirus expressed full-length ERα (PanVera), using methods reported earlier (29, 41).

Mutagenesis and Fluorescent ER Preparations

Cysteine-to-serine mutations at positions 381, 417, and 530 were introduced in a pET-15b human ERα-LBD construct (304–554) using Stratagene QuikChange Site-Directed Mutagenesis Kit with *Pfu* Turbo DNA polymerase and the appropriate oligonucleotides. The corresponding C-to-S ERα-LBD constructs were subcloned in *Nde*I/*Bam*HI sites of a newly double-digested pET-15b construct and sequenced. The His_6-tagged ERα-LBDs were expressed from pET-15b vectors in BL21(DE3)pLysS *E. coli* and purified as described previously (29). Site-specific labeling of receptor was accomplished using 30:1 equivalents of cysteine-specific fluorophore to supernatant [^{3}H]E_2 binding activity while the purified His_6-tagged ERα-LBD was still immobilized on the Ni-NTA resin. The labeling reaction was incubated overnight at 4 C in Tris-glycerol (50 mM Tris, 10% glycerol) pH 7.0 buffer, in the presence of 0.1–0.5 mM TCEP. Excess fluorophore was removed by washing the ERα-LBD-bound resin complex before eluting the fluorescent receptor. The level of derivatization was determined by comparing matrix-assisted laser-desorption ionization-mass spectroscopy spectra of unlabeled and labeled receptor.

Scatchard and Fluorescent GST Pull-Down Assays

The binding affinities of the derivatized ERs were determined directly with [^{3}H]E_2 and calculated by Scatchard analysis as described previously (42). The fluorescent GST pull-down studies were conducted using previously described protocols with the following modifications (27). Briefly, GST-His_6-SRC-1 (629–831) construct in pET-15b, generously provided by Dr. David Shapiro, was expressed in BL21(DE3)pLysS *E. coli* and purified using Ni-NTA resin following the same protocol as with the ERα-LBD (29). The purified GST-His_6-SRC-1 was bound to GSH resin and incubated with active fluorescent ERα-LBD in the presence of excess ligand. After 1 h incubation at 4 C, the GSH beads were washed three times, and bound proteins were eluted with 20 μl solution of elution buffer as described previously (27). The 20 μl elution was combined with 580 μl of Tris-glycerol (pH 8.0) buffer, placed in a 5.0 × 5.0-mm quartz fluorescence cuvette, and measured using a Fluorolog II (model IIIc) fluorometer (Jobin Yvon, Inc.). The fluorescein-labeled ***C530*** receptor was excited at 488 nm (2.5-mm slits), and the emission intensity was monitored at 521 nm (2.5-nm slits). The tetramethylrhodamine-labeled ***C417*** receptor was excited at 541 nm, and the emission intensity was monitored at 580 nm under similar conditions.

Kinetic Dimer Dissociation Assay

For the FRET-based monomer exchange assay, the purified, fluorescein (donor)- and tetramethylrhodamine (acceptor)-labeled ERα-LBD preparations were diluted to 55 nM concentrations. A 5-μl solution of 10 μM ligand stock in Tris-glycerol (pH 8.0) buffer was added to a 45 μl solution of 55 nM donor ER placed in separate wells of a black round-bottom 96-well Nunc polypropylene plate, yielding a final donor ER concentration of 50 nM and 1 μM ligand. In a second plate, 25 μl of 10 μM ligand stock were added to a 225-μl solution of 55 nM acceptor ER placed in separate wells, yielding a final acceptor ER concentration of 50 nM and 1 μM ligand. Both plates were incubated at room temperature for 1 h before 200 μl were removed from the acceptor ER wells and the mixture was added to the 50 μl of donor ER-containing wells incubated with the same ligand, yielding a final concentration of 10 nM donor, 40 nM acceptor ER, and 1 μM ligand. After mixing, the 96-well plate was covered with a clear polyolefin sealing tape (Nalge Nunc International, Rochester, NY), and monomer exchange was monitored immediately by following FRET through the decrease, with time in the fluorescein (donor) emission intensity at 530 nm using a Molecular Devices Gemini XS fluorometer. The samples were excited at 485 nm, with a 515-nm cutoff filter in the excitation pathway, and the chamber was temperature controlled at 28 C. The experiments containing coactivator peptides were conducted under similar conditions with final concentration of 6 nM donor, 20 nM acceptor ER, 1 μM ligand, and proper coactivator peptide. The expression and purification of His_6-tagged SRC-1-NR boxes 1–3 (residues 629–831) and synthesis of SRC-1-NR box 2 (residues 683–696) were conducted as described previously (30). Similar monomer exchange experiments were conducted with a 5 nM total ER concentration in cuvettes using a Fluorolog II (model IIIc) fluorometer under

magic-angle (43) conditions. Monomer exchange kinetics observed with both fluorometers were very similar. To reduce any loss of intensity due to nonspecific sticking of protein to cuvettes or plates, a carrier protein (0.3 mg/ml of chicken ovalbumin) was added to all reaction mixtures. The collected data were fitted to a nonlinear regression, one-phase exponential decay function ($y = \text{plateau} + \text{span}^{-t}$), using Prism 3.00. For all experiments, only data sets that could be fitted with an r^2 value greater than 0.95 were used.

Thermodynamic ER Dimer Affinity Assay

For the FRET-based thermodynamic dimer formation assay, a 700-μl solution of 0.1 nM donor-labeled ER (in Tris-glycerol, pH 8.0, buffer and 0.3 mg/ml chicken ovalbumin, with or without 1 μM ligand) was placed in separate tubes. From a serial dilution of acceptor-labeled ER solution, a sample of less than10 μl was removed and mixed with the 700 μl donor ER (<1.5% dilution). Due to the rather slow dissociation rates of receptor dimers, the samples were incubated for 5–8 h at room temperature (in the dark), for reactions to reach equilibrium. A 600-μl solution of each sample was placed into a 5.0 × 5.0-mm quartz fluorescence cuvette and placed into the sample chamber of the Fluorolog II fluorometer. The sample chamber was held at a constant 25 C while the sample was excited at 488 nm (5.0-mm slits), and donor emission was monitored at 521 nm (2.5-nm slits). Each sample was measured until the standard error was below 1%, three emission data points were averaged for each sample, and each sample was prepared in duplicate. The following signal corrections were conducted for each sample: dark counts correction (to correct for any fluctuations in the photomultiplier tube), signal/reference correction (signal divided by a reference signal to correct for fluctuations in light source intensity), and blank subtraction. Percent FRET was calculated based on the donor intensity (22) with the following equation:

$$\%\text{FRET} = [1-(D_a/D_d)] \times 100$$

where D_a is the donor ER intensity in the presence of acceptor ER, and D_d is the donor ER intensity in the absence of acceptor ER. As all the donor ERs form heterodimers with the excess acceptor ERs, the percent FRET reaches a maximum allowing for calculation of equilibrium dimer dissociation constant (K_d). The K_d was calculated based on percent FRET data and free acceptor ER concentration determined according to standard optical spectroscopy data analysis protocols (43). Briefly, the free acceptor ER concentration of each titration point was determined according to:

$$[A_{free}] = A_{total} - \{(\%\ FRET_{rxn}/\%\ FRET_{max}) \times [D_{total}]\}$$

where A_{free} and A_{total} are the concentrations of free and total acceptor ERs, respectively. The $\%FRET_{rxn}$ and $\%FRET_{max}$ are the percent FRET observed for that reaction and the maximum percent FRET observed for that titration series, respectively. The expression $\%FRET_{rxn}/\%FRET_{max}$ is proportional to the fraction of binding sites filled (F_b). Finally, D_{total} is the concentration of donor ER used (0.1 nM), which is fixed constant along with the concentration of ligand (1 μM) in all reactions. The dissociation constant was then determined by fitting the raw %FRET data to a simple single binding site model:

$$F_b = \{((\%\ FRET_{max})[A_{free}])/((K_d) + [A_{free}])\} + C$$

where, C is a constant which is the percent FRET observed in the absence of acceptor ER, which for our case is 0 (43, 44).

Acknowledgments

We would like to thank Dr. Theodore L. Hazlett (Laboratory for Fluorescence Dynamics, Department of Physics, University of Illinois) for his help in calculating equilibrium dissociation constants based on optical spectroscopy data. We would also like to thank past members of our group who synthesized many of the ligands used in this report: Elio Napolitano, Ying R. Huang, Marvin J. Meyers, Deborah S. Mortensen, Donald A. Seielstad, Kwang Jin Hwang, and Shaun R. Stauffer.

Received July 16, 2002. Accepted September 9, 2002.

Address all correspondence and requests for reprints to: John A. Katzenellenbogen, Department of Chemistry, University of Illinois, 600 South Mathews Avenue, Urbana, Illinois 61801. E-mail: jkatzene@uiuc.edu.

This work was supported by a grant from the NIH (PHS 5R37 DK-15556).

REFERENCES

1. Mangelsdorf DJ, Thummel C, Beato M, Herrlich P, Schutz G, Umesono K, Blumberg B, Kastner P, Mark M, Chambon P 1995 The nuclear receptor superfamily: the second decade. Cell 83:835–839
2. Olefsky JM 2001 Nuclear receptor minireview series. J Biol Chem 276:36863–36864
3. Lees JA, Fawell SE, White R, Parker MG 1990 A 22-amino-acid peptide restores DNA-binding activity to dimerization-defective mutants of the estrogen receptor. Mol Cell Biol 10:5529–5531
4. Brzozowski AM, Pike AC, Dauter Z, Hubbard RE, Bonn T, Engström O, Öhman L, Greene GL, Gustafsson J-A, Carlquist M 1997 Molecular basis of agonism and antagonism in the oestrogen receptor. Nature 389:753–758
5. Schwabe JWR, Chapman L, Finch JT, Rhodes D 1993 The crystal structure of the estrogen receptor DNA-binding domain bound to DNA: how receptors discriminate between their response elements. Cell 75:567–578
6. Salomonsson M, Häggblad J, O'Malley BW, Sitbon GM 1994 The human estrogen receptor hormone binding domain dimerizes independently of ligand activation. J Steroid Biochem Mol Biol 48:447–452
7. Brandt ME, Vickery LE 1997 Cooperativity and dimerization of recombinant human estrogen receptor hormone-binding domain. J Biol Chem 272:4843–4849
8. Tanenbaum DM, Wang Y, Williams SP, Sigler PB 1998 Crystallographic comparison of the estrogen and progesterone receptors ligand binding domains. Proc Natl Acad Sci USA 95:5998–6003
9. Wang H, Peters GA, Zeng X, Tang M, Ip W, Khan SA 1995 Yeast two-hybrid system demonstrates that estrogen receptor dimerization is ligand-dependent *in vivo*. J Biol Chem 270:23322–23329
10. Erijman L, Weber G 1993 Use of sensitized fluorescence for the study of the exchange of subunits in protein aggregates. Photochem Photobiol 57:411–415
11. Waggoner A 1995 Covalent labeling of proteins and nucleic acids with fluorophores. Methods Enzymol 246: 362–373
12. Hegy GB, Shackleton CHL, Carlquist M, Bonn T, Engstrom O, Sjoholm P, Witkowska HE 1996 Carboxymethylation of the human estrogen receptor ligand-binding domain-estradiol complex: HPLC/ESMS peptide mapping shows that cysteine 447 does not react with iodoacetic acid. Steroids 61:367–373
13. Goldstein SW, Bordner J, Hoth LR, Geoghegan KF 2001 Chemical and biochemical issues related to X-ray crystallography of the ligand-binding domain of estrogen receptor α. Bioconjug Chem 12:406–413
14. Reese JC, Katzenellenbogen BS 1992 Characterization of a temperature-sensitive mutation in the hormone bind-

ing domain of the human estrogen receptor: studies in cell extracts and intact cells and their implications for hormone-dependent transcriptional activation. J Biol Chem 267:9868–9873
15. Stoica A, Pentecost E, Martin MB 2000 Effects of selenite on estrogen receptor α expression and activity in MCF-7 breast cancer cells. J Cell Biochem 79:282–292
16. Neff S, Sadowski C, Miksicek R 1994 Mutational analysis of cysteine residues within the hormone-binding domain of the human estrogen receptor identifies mutants that are defective in both DNA-binding and subcellular distribution. Mol Endocrinol 8:1215–1223
17. Reese JC, Katzenellenbogen BS 1991 Mutagenesis of cysteines in the hormone binding domain of the human estrogen receptor: alterations in binding and transcriptional activation by covalently and reversibly attaching ligands. J Biol Chem 266:10880–10887
18. Gangloff M, Ruff M, Eiler S, Duclaud S, Wurtz JM, Moras D 2001 Crystal structure of a mutant hERα ligand-binding domain reveals key structural features for the mechanism of partial agonism. J Biol Chem 276:15059–15065
19. Reese JC, Wooge CH, Katzenellenbogen BS 1992 Identification of two cysteines closely positioned in the ligand binding pocket of the human estrogen receptor: roles in ligand binding and transcriptional activation. Mol Endocrinol 6:2160–2166
20. Seielstad DA, Carlson KE, Kushner PJ, Greene GL, Katzenellenbogen JA 1995 Analysis of the structural core of the human estrogen receptor ligand binding domain by selective proteolysis/mass spectrometric analysis. Biochemistry 34:12605–12615
21. Seielstad DA, Carlson KE, Katzenellenbogen JA, Kushner PJ, Greene GL 1995 Molecular characterization by mass spectrometry of the human estrogen receptor ligand-binding domain expressed in *Escherichia coli.* Mol Endocrinol 9:647–658
22. Selvin PR 1995 Fluorescence resonance energy transfer. Methods Enzymol 246:300–334
23. Stauffer SR, Huang YR, Aron ZD, Colleta CJ, Sun J, Katzenellenbogen BS, Katzenellenbogen JA 2001 Triarylpyrazoles with basic side chains: development of pyrazole-based estrogen receptor antagonists. Bioorg Med Chem 9:151–161
24. Mortensen DS, Rodriguez AL, Carlson KE, Sun J, Katzenellenbogen BS, Katzenellenbogen JA 2001 Synthesis and biological evaluation of a novel series of furans: ligands selective for estrogen receptor α. J Med Chem 44:3838–3848
25. Mortensen DS, Rodriguez AL, Sun J, Katzenellenbogen BS, Katzenellenbogen JA 2001 Furans with basic side chains: synthesis and biological evaluation of a novel series of antagonists with selectivity for the estrogen receptor α. Bioorg Med Chem Lett 11:2521–2524
26. Bindal RD, Carlson KE, Reiner GC, Katzenellenbogen JA 1987 11β-Chloromethyl-[^{3}H]estradiol-17β: a very high affinity, reversible ligand for the estrogen receptor. J Steroid Biochem 28:361–370
27. Kraichely DM, Sun J, Katzenellenbogen JA, Katzenellenbogen BS 2000 Conformational changes and coactivator recruitment by novel ligands for estrogen receptor-α and estrogen receptor-β: correlations with biological character and distinct differences among SRC coactivator family members. Endocrinology 141:3534–3545
28. Meyers MJ, Sun J, Carlson KE, Katzenellenbogen BS, Katzenellenbogen JA 1999 Estrogen receptor subtype-selective ligands: asymmetric synthesis and biological evaluation of *cis*- and *trans*-5,11-dialkyl-5,6,11,12-tetrahydrochrysenes. J Med Chem 42:2456–2468
29. Carlson KE, Choi I, Gee A, Katzenellenbogen BS, Katzenellenbogen JA 1997 Altered ligand binding properties and enhanced stability of a constitutively active estrogen receptor: evidence that an open pocket conformation is required for ligand interaction. Biochemistry 36: 14897–14905
30. Gee AC, Carlson KE, Martini PGV, Katzenellenbogen BS, Katzenellenbogen JA 1999 Coactivator peptides have a differential stabilizing effect on the binding of estrogens and antiestrogens with the estrogen receptor. Mol Endocrinol 13:1912–1923
31. Yudt MR, Koide S 2001 Preventing estrogen receptor action with dimer-interface peptides. Steroids 66: 549–558
32. Shiau AK, Barstad D, Loria PM, Cheng L, Kushner PJ, Agard DA, Greene GL 1998 The structural basis of estrogen receptor/coactivator recognition and the antagonism of this interaction by tamoxifen. Cell 95:927–937
33. Sack JS, Kish KF, Wang C, Attar RM, Kiefer SE, An Y, Wu GY, Scheffler JE, Salvati ME, Krystek SR, Weinmann R, Einspahr H 2001 Crystallographic structures of the ligand-binding domains of the androgen receptor and its T877A mutant complexed with the natural agonist dihydrotestosterone. Proc Natl Acad Sci USA 98:4904–4909
34. Peters GA, Khan SA 1999 Estrogen receptor domains E and F: role in dimerization and interaction with coactivator RIP-140. Mol Endocrinol 13:286–296
35. Dauvois S, Danielian PS, White R, Parker MG 1992 Antiestrogen ICI164,384 reduces cellular estrogen receptor content by increasing its turnover. Proc Natl Acad Sci USA 89:4037–4041
36. Pike ACW, Brzozowski AM, Walton J, Hubbard RE, Thorsell A, Gustafsson JA, Carlquist M 2001 Structural insights into the mode of action of a pure antiestrogen. Structure 9:145–153
37. Bramlett KS, Yifei W, Burris TP 2001 Ligands specify coactivator nuclear receptor (NR) box affinity for estrogen receptor subtypes. Mol Endocrinol 15:909–922
38. Margeat E, Poujol N, Boulahtouf A, Chen Y, Muller JD, Gratton E, Cavailles V, Royer C 2001 The human estrogen receptor α dimer binds a single SRC-1 coactivator molecule with an affinity dictated by agonist structure. J Mol Biol 306:433–442
39. Nolte RT, Wisely GB, Westin S, Cobb JE, Lambert MH, Kurokawa R, Rosenfeld MG, Willson TM, Glass CK, Milburn MV 1998 Ligand binding and co-activator assembly of the peroxisome proliferator-activated receptor-γ. Nature 395:137–143
40. Napolitano E, Fiaschi R, Carlson KE, Katzenellenbogen JA 1995 11β-Substituted estradiol derivatives 2: potential carbon-11 and iodine-labeled probes for the estrogen receptor. J Med Chem 38:2774–2779
41. Katzenellenbogen JA, Johnson Jr HJ, Myers HN 1973 Photoaffinity labels for estrogen binding proteins of rat uterus. Biochemistry 12:4085–4092
42. Scatchard G 1949 The attractions of proteins for small molecules and ions. Ann NY Acad Sci 51:660–672
43. Tetin SY, Hazlett TL 2000 Optical spectroscopy in studies of antibody-hapten interactions. Methods 20: 341–361
44. Tetin SY, Rumbley CA, Hazlett TL, Voss EW 1993 Elucidation of anti-ssDNA autoantibody BV 04–01 binding interactions with homooligonucleotides. Biochemistry 32:9011–9017